The Johns Hopkins University
APPLIED PHYSICS LABORATORY
Silver Spring, Maryland

STELLAR PHOTOMETRY FROM A SATELLITE VEHICLE

Andrew M. Smith

Applied Physics Laboratory

The Johns Hopkins University

December 1965

This research was supported in part by the Bureau of Naval Weapons, Department of the Navy under contract NOw 62-0604-c and in part by the National Aeronautics and Space Administration.

The Johns Hopkins University
APPLIED PHYSICS LABORATORY
Silver Spring, Maryland

ABSTRACT

23722

Data acquired from a satellite borne telescope-photometer sensitive to far ultraviolet radiation is presented. The telescopic field of view was about π square degrees; the effective photometer band width and wavelength were 204Å and λ1376Å respectively. Assuming $A_V/E(B-V) = 3.1$ and $E(B-V) = 1$ an average extinction at λ1376Å of 10.7 ± 6 mag. was found from the data. An ultraviolet color index, $(m_{1376} - V)$, corrected for interstellar absorption was computed for 96 stars, and from these data together with a set of unblanketed model atmospheres the derivation of a temperature scale was attempted. The results indicate a scale from 2000 to 3000 degrees lower than currently estimated. The effect of using a more appropriate line blanketed model for these purposes is briefly discussed. AUTHOR

INTRODUCTION

The desirability from an astrophysical standpoint of measuring stellar ultraviolet fluxes at wavelengths less than 3000Å, or below the lower limit of atmospheric transmission, is quite generally recognized, and to date several attempts have been made via rocket vehicles to secure such data (e.g., Alexander, Bowen, and Heddle, 1963; Chubb and Byram, 1963; Stecher and Milligan, 1962). In an effort to augment these results by an extensive scan of the celestial sphere, two telescope-photometers were mounted on board satellite 1964 83C and launched into a nearly circular polar orbit at about 1100 km altitude in December 1964. Thus, situated well above the earth's atmosphere the photometers executed a slow uncontrolled scan of the earth and sky in which all pointing directions were possible. For both photometers the optics defined a circular field of view of about π square degrees. The primary purpose of one photometer was to record stellar fluxes in the band λ1297Å to λ1650Å, and the preliminary results of these measurements are reported herein.

SATELLITE DESCRIPTION

The satellite was magnetically stabilized and carried with the photometers a Rubidium vapor magnetometer, two omni-directional particle radiation detectors, and several experiments designed primarily to afford useful engineering data. Figure 1 is a simplified drawing of the satellite in which the deployment of the principal components is illustrated. The optical axes of the telescopes were oriented normal to the satellite magnetic axis and thus in orbit were roughly normal to the local geomagnetic field vector.

The dynamic behavior of the satellite was in general composed of a rotation imparted by the geomagnetic field, a rotation about the satellite magnetic axis and a precession with a superimposed nutation of the magnetic axis about the geomagnetic field vector. The complicated nature of the satellite's motion makes theoretical predictions of the telescope attitudes over an extended period of time very difficult. In principle, however, it is possible to determine the attitude at relatively short time intervals knowing the magnetic field and sun vectors in a satellite fixed coordinate system together with the components of these same vectors in a convenient geocentric coordinate system. To this end a satellite cartesian coordinate system was established using a number of solar attitude detectors (labeled in Figure 1 "Heliogoniometers") which were able to locate the sun vector to within 0.1 degree. Three vector magnetometers were mounted as nearly as possible parallel to the satellite axes. Making use of all attitude data together with theoretical values of the geomagnetic field (Cain, Daniels, Hendricks, and Jensen, 1965) the stellar

aspect could be determined with an accuracy of about 1/2 to 1 1/2 degrees. Telescope pointing information is, of course, unavailable by this method when the sun is lost to view from the satellite. As of now no attempt has been made to recover this information by an analysis of the satellite's dynamic behavior.

The angular velocity of the telescope optical axes decreased from an initially high value to about 1/5 degree per second. Commensurate with this slow scanning speed the photometer responses were integrated over a period of 1.23 seconds and were continuously transmitted every 1.31 seconds over a PCM channel at the rate of 195.3 bits per second. The channel capacity for each photometer was 15 bits of digital information.

Electrical power was provided by an array of solar cells in conjunction with Nickel-Cadmium batteries. In minimum or near minimum sun conditions it became necessary to duty cycle the photometer experimental package. This unfortunate circumstance, however, effected only the quantity and not the quality of photometric data.

Telemetry reception was carried out by a network of NASA and APL stations; and, finally, tracking, attitude determinations, and data reduction were performed by the Applied Physics Laboratory.

THE EXPERIMENT

A drawing of the photometer unit appears in Figure 2. Here is shown the disposition of the optical systems, the photometer detectors, a particle background detector, an in-flight calibration mechanism, and necessary shielding. An exploded view illustrates in greater detail a photometer detector assembly. The associated electronics were mounted above the illustrated unit in such a way that the electronics and the photometer comprised a completely self contained experimental package. In Table I are listed the pertinent characteristics of both photometers and the background detector.

Except for the filters the telescope optical systems were as identical as possible. A Newtonian optical system was employed with an aperture of 2 5/8 inches and an f number of 2.29. The mirrors were aluminized and overcoated with MgF_2 in the manner of Hass and Tousey (1959). As a result, a reflectivity to Lyman-α radiation at normal incidence of 78% was achieved. This value is based on the measured reflectivity of a plane mirror which was coated simultaneously with the telescope mirrors. For each telescope the total angular field of view as defined by a circular aperture in the focal plane was approximately 2 degrees. Light, having passed through the aperture encountered a crystal filter of either LiF or SrF_2 depending upon the photometer in question. These filters defined lower wavelength limits to the transmitted radiation of 1050Å and 1297Å respectively. Since no precaution against exposure to sunlight was taken the filters were displaced from the Newtonian focus as far as possible to avoid damage from local heating.

Bendix resistance strip magnetic electron multipliers, Model number M310, were used as detectors. The "volume" photoelectric emission characteristics of the Tungsten photocathodes determined the long wavelength threshold of the photometer response, this latter quantity being about 1650Å. The photometers were operated in the pulse counting mode at gains of about 10^6. Each photomultiplier was followed by an amplifier-discriminator combination, the output of which led directly to the interface electronics. Details concerning the operation of these resistance strip electron multipliers have been reported elsewhere (Heroux and Hinteregger 1960; Goodrich and Wiley 1961). Relative to their use in the case at hand it is simply noted that for certain photomultiplier dynode strip voltages and amplifier gains a reasonably well defined plateau will occur in a graph showing the integral count as a function of the dynode strip voltage. The photomultipliers were operated in this plateau region in such a way that a change of 50 volts in either the dynode or field strip voltages would cause at most a 3.3% change in the integral counting rate. The photomultiplier voltages were supplied with a long term stability better than 1.0% or to within a fluctuation of ± 9.0 volts at the most. Thus, uncertainties in the counting rates due to changes in the photomultiplier voltages were considered negligible.

Since the experimental package was to be exposed to intense particle radiation in the trapped radiation zones, brass shielding about 1/4 inch thick surrounded almost entirely each combination of photomultiplier, crystal filter and focal plane aperture, leaving a cone shaped opening for the entering radiation. In addition, a background detector was included identical mechanically in every way to the photometer detector assemblies and oriented

in an equivalent position relative to the local geomagnetic field. The background detector differed from the photometers in as far as it lacked an associated primary and secondary mirror system, thus creating a slightly different shielding configuration. An aluminum filter located in the background detector in a position corresponding that of the crystal filters in the photometers was designed to compensate as much as possible for this difference. The electron and proton transmission characteristics of the aluminum filter and thus the threshold sensitivities of the background detector to these particles are listed in the last column of Table I.

Provision was made for a simple in-flight calibrator which was in essence a small Cerenkov radiator with a mechanical shutter to regulate the emission of light. The radiator was constructed by simply holding two line sources of Sr^{90}, contained in an aluminum block, close to two LiF crystals. Electrons stopping in the crystals generated ultraviolet radiation which could pass through the crystals and into the optical system. The calibrator was located at the front of the photometer package in such a way that light from one half of the calibrator entered one telescope and light from the other half entered the adjacent telescope. Because of this arrangement a single solenoid operated shutter could be used to calibrate both systems. The calibrator afforded a limited usefulness, however, for a large fraction of the ultraviolet light generated was lost in the optical systems before reaching the photomultipliers. As a result, the response of the stellar photometer, that is, the one employing a SrF_2 filter, to the calibrator radiation alone was roughly comparable to the background signal. Nevertheless this photometer yielded useful information when under calibration. In

the case of the LiF filtered photometer, however, the calibrator induced response was completely lost in the signal generated by the ubiquitous Lyman-α sky glow.

Relative and absolute photometer sensitivities were made at the National Bureau of Standards on one photomultiplier in combination with either a LiF or SrF_2 filter. A sodium salicylate coated photomultiplier with an approximately constant quantum efficiency (Samson 1964) was used in the usual manner to monitor the monochromator beam intensity. The relative dependence of sensitivity on wavelength was determined by comparing the monitor output with the photometer detector response. The absolute sensitivity was measured using a Nitric Oxide ion chamber as a means of calibrating the monochromator at $\lambda 1254\text{Å}$. An ionization efficiency of 74% (Watanabe 1954) was assumed.

After the flight experimental package had been launched into orbit, a nearly identical alternate unit was calibrated at the NASA Goddard facilities. In this measurement the entire experimental package was located in a beam of parallel monochromatic ultraviolet light. The beam intensity was determined using a calibrated EMR 542F08 photomultiplier, and once again a sodium salicylate coated photomultiplier was used to establish the relative sensitivity. Results from this measurement indicated an instrumental sensitivity reduced by a factor of 1.7 from the original value determined before launch. It is believed that the second method of calibration contained fewer uncertainties than the first, and consequently the absolute value of the photometer sensitivity was revised accordingly.

Relative photometer detector performances for other photomultiplier-filter combinations were determined at APL using a Cerenkov radiator similar to that described for use as an in-flight calibration mechanism. It was found that sufficiently large counting rates were obtained when a photometer-filter combination was exposed directly to a calibrator utilizing a 10 microcurrie source of Sr^{90}. Under these circumstances, negligible fatigue was observed in the Cerenkov radiator.

Figure 3 shows the results of these measurements for the orbited photometers. The graph labeled B exhibits the dependence of the system sensitivity upon wavelength for both the LiF and the SrF_2 filtered photometers. In the latter case the sensitivity function is shown again on a larger scale in the graph labeled A. Because of the width of the sensitivity function there was a variation in the effective wavelength and sensitivity with stellar type. Using the model atmospheres of Mihalas (1964) the total change in effective sensitivity corresponding to a variation in effective temperature from 45,000°K to 9,000°K was found to be less than 4.5%. This small variation was taken into account in the data reduction computations. For the same temperature range the effective wavelength changes by about 12Å. The values for these quantities appearing in Table 1 are the average effective wavelength, 1376Å, and the corresponding effective sensitivity.

A cross talk problem existed such that detection events in the background detector effected the counting rates in both photometers. This effect was temperature dependent but never exceeded 9.2% as measured in the laboratory. In practice the maximum observed cross talk contribution to the stellar photometer response during star detection events was 16 counts per accumulation period. By

comparison the photometer response to stars alone was from 3 to 960 times this number, and for a large majority of cases the cross talk contribution was completely negligible. Because of the slowly varying behavior with time of this as well as other contributions to the background signal, corrections could be made by simple extrapolation procedures. Consequently, uncertainties arising from this problem are considered unimportant.

The average temperature of the photometers and background detector was 71°F differing from this value by no more than ± 11°F during the period of data aquisition. Based on laboratory measurements, no significant variations in the photometer or background detector responses can be caused by these temperature fluctuations.

The experimental package was subjected to the usual vibration tests conducted in order to evaluate the effects of the rocket launching on the equipment performance. No measurable change in the optical system was observed. Previous to these tests all the electronic components including the photomultipliers were subjected to similar checks. While the circuitry was unaffected the photomultipliers enjoyed no such immunity. Not only did the apparent detection efficiency to both electromagnetic and particle radiation change, but it did so in as many different ways as there were photomultipliers. The photomultipliers used in the orbited experimental package were those effected least by simulated launch conditions. The maximum observed sensitivity fluctuation after several vibration tests was in the case of the photometers 1.4%; in the case of the background detector 2.4%. Of course, while it is impossible to know the final effect of the

launch upon the photometer and background detector sensitivities it seems reasonable to expect that changes in the sensitivities from this source will be less than ± 5% of the prelaunch values.

THE RESULTS

Representative histograms of the raw data appear in Figure 4. The abscissa is divided into units of twice the photometer accumulation period, and the number of counts recorded during the accumulation period is plotted on the ordinate. In general, as is illustrated by the response diagrams, a star was in the field of view for a time sufficiently long to permit integration of the signal several times. From this data an average integrated count could be found which was subsequently used in the determination of a stellar flux value. Conversely, the shape of a photometer response indicated unambiguously whether or not a star had been completely in the photometer field of view.

The background contribution to the photometer signal could be separated into two categories; the first being composed of undesirable sources roughly comparable to the stellar response of interest both in duration and in magnitude; the second including those contributions which varied slowly with time and usually were much smaller in magnitude than the stellar signals. In the first category were telemetry noise bursts which could be identified by inspection. Included also were those hot stars which entered the field of view along with the source responsible for the major part of the observed response. Sometimes this latter type of background contribution could be eliminated on the basis of timing considerations, but usually it could not be eliminated at all. For such cases in which the secondary source was considerably fainter than the primary one the uncertainty in the results included an estimate of the photometer response due to the

secondary source alone. More often than not, however, the entire star detection event was discarded.

In the realm of the second category is light from faint hot stars integrated over the field of view, light from extended sources near the earth, scattered sunlight in the photometer itself and as mentioned previously the very small contribution from cross talk between the background detector and either photometer. The ν Sco response pictured in Figure 4 exhibits a relatively high background signal typical of that due to sunlight scattered in the photometer. For these sources the magnitude of the background was estimated by simply extrapolating the background signal underneath the stellar response as illustrated in Figure 4 by the dashed lines. The correction was made by simply subtracting the estimated background signal from the total average signal. Except for faint stars the uncertainty in this procedure was less than the observed fluctuations of the total signal which were in general somewhat greater than to be expected statistically. It is strongly suspected that beyond effects due to the appearance and disappearance from the field of view of faint stars there are fluctuations in the signal induced by inhomogeneities in the SrF_2 filter.

While it was difficult to differentiate between the causes of signal fluctuations it was possible to take account of these fluctuations in the flux value uncertainty estimates. In cases where the fluctuation in the total signal was less than that to be expected statistically the composite standard deviation, calculated from both the total and estimated background counting rates, was added to the uncertainty associated with the position of the extrapolated background level. In cases where the photometer signal

fluctuations exceeded statistical expectations the maximum observed deviation was substituted for the standard deviation of the total signal. A lower limit to the uncertainties in relative flux values of 10% was considered realistic and therefore has been adopted.

During calibration events the photometers received radiation from the calibrator for usually five accumulation periods. After background corrections were made the counts in each accumulation period were averaged and the result in turn was averaged with similar results from calibrations carried out during the same day. In Figure 5 this corrected photometer response is plotted as a function of day number for a 118 day period following launch. The bars on a few of the points indicate the size of the standard deviation. The solid line which has been normalized to the data of day 35 represents the results of a similar calibration procedure carried out in the laboratory on an alternate model of the photometer package. In addition to poor counting statistics, the fluctuating background signal accounts for the dispersion in the flight photometer data. The decay in the ground based photometer response is considered principally due to crystal degradation in the calibrator. The decay of the flight photometer response is if anything less than that of the ground based unit, and is thought to arise from the same cause. Thus, effects such as decreases in the mirror reflectivity or the SrF_2 filter transmission, or changes in the detection efficiency of an electronic nature are excluded. That is, the calibration results indicate that the stellar photometer sensitivity did not change over the 118 day period following launch.

Fortunately, an additional check on this conclusion was available. During the course of gathering data the photometer made multiple detections of the same star for 32 different stars. In Figure 6 some of these stars are plotted as points on a flux vs. day diagram. The bars indicate the uncertainty in the stellar flux values. Apart from a visual inspection of the diagram a simple estimate of a change in the photometer sensitivity may be made by averaging the observed changes in flux values between the 10 stars of Figure 6. The result of this procedure is an average net change with time toward smaller flux values of 0.6% during the 84 day period covered by the measurements. In view of the foregoing evidence it is felt that the stellar photometer sensitivity was constant to within 5%. In addition, a 50% uncertainty is attributed to the stellar flux absolute values.

Table 2 contains the photometry results for 96 stars. Columns 1, 2, and 3 contain a running number, the HD number, and the star name respectively. The spectral classifications are listed in column 4. Morgan-Keenan types are used preferentially; otherwise recourse is made to the HD spectral classifications. Column 5 contains the apparent visual magnitude in the UBV system except where noted, and column 6 contains the B-V color indices. References to the data of columns 4, 5, and 6 appear in column 7. The values of v sin i, the observable component of the rotational velocity, are recorded in column 8 and are all taken from the articles of Slettebak (1949, 1954, 1955, 1956). In column 9 are listed the values of the stellar flux, F(1376), at the effective wavelength of $\lambda 1376\text{Å}$. An extreme ultraviolet color index $(m_{1376} - V)_u$ is listed in column 10. These values are uncorrected for reddening and are calculated from the formula

$$(m_{1376} - V)_u = -2.5 \log F(1376)/F(5475) \qquad (1)$$

where F(5475) is the monochromatic flux at $\lambda 5475\mathring{A}$. In making the computations it was assumed; (a) that $\lambda 5475\mathring{A}$ was the effective wavelength defined by the V filter of the UBV system for B type stars, and (b) that a star of V = 0 delivers to the earth above the atmosphere a flux of 4.0×10^{-9} ergs cm^{-2} sec^{-1} $\mathring{A}^{-1}$ at $\lambda 5475\mathring{A}$ (Code 1960). The numbers appearing in the last column of Table 2 indicate the number of times the corresponding star was detected, the letters refer to notes at the end of the Table.

In order to make corrections for interstellar absorption the relationship between $E(m_{1376} - V)$ and E(B-V) was assumed to be a linear one. That is

$$E(m_{1376} - V) = XE(B - V). \tag{2}$$

Using this equation the value of X was determined for eight pairs of stars, those in each pair being of the same spectral type and luminosity class. Listed in Table 3 are the stars selected for the calculation of X, their classifications and the corresponding values of X where the intrinsic (B-V) colors are taken from Johnson (1963) and the other necessary quantities from Table 2. An overall average in which equal weight is attributed to each X-value of Table 3 is

$$X_{avg} = 7.6 \pm 0.8 \text{ (S.D.)}. \tag{3}$$

No attempt was made in any of the calculations to identify different values of X with different regions of the sky. Accordingly, X_{avg} was used to correct all data for interstellar absorption by means of relation (2), and the new values for the extreme ultraviolet colors $(m_{1376} - V)$ appear in column 11 of Table 2.

It is interesting to compare these results with those of Boggess and Borgman (1964). Under the conditions that $A_V/E(B - V) = 3.1$ and $E(B - V) = 1$ mag. the extinction at $\lambda 1376\text{Å}$ as measured in the present experiment is 10.7 ± 0.6 (p.e.). Figure 7 exhibits this quantity together with the data appearing in the paper of Boggess and Borgman. Plotted also is the dielectric grain extinction curve No. 15 of van de Hulst (1949). Clearly the value determined herein for E(1376) confirms the trend in the far ultraviolet to larger extinction than that indicated by the illustrated theoretical relationship. Recent measurements of the interstellar extinction carried out at 15 different wavelengths by Stecher (1965) together with extinctions at $\lambda 1314\text{Å}$ $\lambda 1427\text{Å}$ calculated by Stecher from the data of Chubb and Byram demonstrate in greater detail the same general spectral behavior. The agreement between Stecher's value for the extinction in the neighborhood of $\lambda 1376\text{Å}$, approximately 10, and the value quoted in the present paper is well within the estimated experimental uncertainties.

In recognizing the need for a dielectric material to increase the extinction above the van de Hulst values at short wavelengths, two explanations for these observations have been put forth. One of these based on the suggestion of Wickramasinghe (1963) relegates the role of scattering agent to composite carbon core-ice mantle grains. In another approach Stecher and Donn (1965) have focused attention on the dielectric properties of graphite crystals arising out of their anisotropic character. By assuming a random orientation of graphite crystals in space these authors suggest that the observed extinction may be accounted for by carbon grains alone.

In Figure 8 are plotted the ultraviolet colors ($m_{1376} - V$) of stars for which the apparent visible magnitude V and the B - V color

index were available. The numbers beside a point identify a star by means of the running number of Table 2. The dashed lines illustrate theoretical expectations based on the temperature scale of Harris (1963), and computed from the model atmospheres of Mihalas in conjunction with the photometer sensitivity function. While some of the spread in $(m_{1376} - V)$ within a spectral class can be explained in terms of the counting statistics there appears to be an intrinsic dispersion as well. Those stars, designated by triangles, with v sin $i \geq 220$ km sec^{-1} exhibit $(m_{1376} - V)$ colors preferentially more positive than the average except in three cases: No. 1, γ Cas; No. 91, ξ Oph; and No. 64, p Car. Although there is apparently no value of v sin i for stars numbered 1, 64, and 95 (λ Pav) all are emission stars and are assumed to be rotating close to their critical velocities. The results of Collins (1965) indicate that in the case of a star with a mass of $8M_\odot$, a polar radius of $4R_\odot$, and a rotational velocity of $0.8\,\omega_c$ one might expect a change in $(m_{1376} - V)$ to a more positive value relative to the case in which $\omega = 0$ of about 0.24 mag. When the angular velocity equals the critical angular velocity the corresponding change in $(m_{1376} - V)$ is about 1.27 mag. This implies that those rotating stars which do appear to be represented by $(m_{1376} - V)$ colors more positive than the average are rotating with velocities close to their critical values. The anomalous character of the exceptions No. 64, p Car and No. 1 γ Cas does not seem to be altered by the uncertainty in their $(m_{1376} - V)$ colors, and it is simply noted that both are emission stars, the latter being a shell star as well.

The circles appearing in Fig. 8 represent stars of luminosity classes I and II. Again the relatively more positive values of $(m_{1376} - V)$ for stars No. 50, ι CMa, B3 II and No. 52, γ CMa, B8 II probably reflect a low value for

log g. Stars numbered 38 and 41 are ξ and ε Ori respectively, and since the ratio $R = A_v/E(B - V)$ in the Orion belt region is known to be different from the normal value (Johnson 1965) it is likely that the correction for absorption between these stars and earth is inadequate; thus, their anomalously positive $m_{1376} - V$ colors cannot be thought exclusively due to low surface gravities.

In Table 4 are listed 36 stars from which a mean $(\overline{m_{1376} - V})$ color index was determined for each of 12 spectral types. The weight of each datum was inversely proportional to the square of its standard deviation, and the quoted uncertainty is the standard deviation in the weighted mean. Ideally, only stars of luminosity classes IV and V and low v sin i values were used. Because of the paucity of data, however, some compromises were made in this respect. Thus, there was only one star available in classes B9, B6, and 09.5 the latter being No. 36, δ Ori of luminosity class II. In addition, many of the values of v sin i for stars which were used in the averaging process are unknown.

By making recourse again to the models of Mihalas effective temperatures may be found corresponding to the mean $(\overline{m_{1376} - V})$ color indices. Following Harris the quantity $10^4/T_e$ is plotted as a function of the $(B - V)_o$ color index in Figure 9, and a least squares fit to a straight line is obtained using data for types B0.5 through B9. For these types smoothed values of T_e may be determined. In addition, an estimate of the effective temperature for an A0 star was made by simply extrapolating the straight line fit to $(B - V)_o = 0$. The effective temperature for O7, 09.5, and B0 stars were calculated directly from the appropriate $(\overline{m_{1376} - V})$ color index. These results which with the exception of spectral classes O7 and 09.5 are intended to represent

luminosity types IV and V are listed in Table 5 together with those of Harris; they were also used in generating the solid curve in Figure 8. The uncertainty in effective temperatures for types O7, O9.5, B0, and B0.5 are derived directly from the standard deviation in the weighted mean ($\overline{m_{1376} - V}$) color index. Similar calculations were made for types B1 through B9 and the results were average to produce an uncertainty of ± 500°K. It would seem that for the types B1, B2, and B3 an uncertainty of about ± 700°K would be more appropriate; as could have been expected the experiment was singularly insensitive to variations in the temperature parameter for the high temperature models. For types A0 through B1 the temperatures determined herein are from 2000 to 3000 degrees less than those of Harris, but are in good agreement with the temperatures reported by Stecher (1964). The extrapolated value of T_e = 8,800°K for type A0 stars is 400°K less than the temperature attributed to Vega by Hanbury Brown, Hazard, Davis and Allen (1964). The theoretical value of (m_{1376} - V) corresponding to T_e = 9200°K is shown by a diamond symbol in Fig. 8. This discrepancy is within an estimated standard deviation of ± 500°K. However, it may be noted in passing that a redetermination of the bolometric correction for Vega taking into account the effect of line blanketing in the far ultraviolet might lead to a more positive bolometric magnitude than used by the preceding authors and thus a lower effective temperature.

Likewise, for a B1.5 V star an interpolated value for T_e of 20,400°K is estimated whereas Mihalas and Morton (1965) have derived a model of a B1.5 V star with line blanketing for which T_e = 21914°K. Using this model and the photometer sensitivity function a value of -3.80 mag. was calculated for (m_{1376} - V) which is shown again by a diamond symbol in Figure 8 at type

B1.5. This theoretical (m_{1376} - V) color falls close to the observed colors for stars of types close to B1.5, and the difference of approximately 1500°K between the interpolated value and the theoretical value of T_e probably reflects to some degree the experimental error as well as the error made in the smoothing procedure. In reference to the work of Mihalas and Morton, the question arises as to what the effect would be if the present comparisons were based on the use of models incorporating line blanketing instead of those which did not. Using the blanketed model as a guide it is estimated that the effective temperatures would be increased over those determined from the unblanketed models from 700 to 800 degrees for stellar types B1 and B2. Unfortunately, the present experiment is unable to indicate whether or not one should expect the effect of line blanketing to be greater or smaller than that deduced from the model of Mihalas and Morton. This insensitivity arises in part from the rather broad photometer sensitivity function which includes both deletions and additions to the unblanketed model flux and in part from uncertainty in the absolute value of the photometer sensitivity. Nevertheless, the modification in the present theoretical (m_{1376} - V) colors resulting from the use of a line blanketed model is in the direction of closer agreement with observation, and it is surmised that the introduction of line blanketed models into the analysis would result in stellar temperatures higher by amounts on the order of the presently quoted uncertainties.

It is, of course, impossible to acknowledge all those who have contributed significantly to the completion of this experiment. Asking the indulgence of those whose names I omit, I would particularly like to recognize the work of the following persons. Mr. D. S. Beall was responsible for a

large part of the work connected with the use and calibration of the photo-multipliers. Mr. H. P. Lie supervised the design and construction of the necessary electronic components as well as the environmental test procedures. The solution of the attitude problem was due largely to the efforts of Messrs. H. D. Black and G. B. Bush with a considerable portion of the programming responsibilities for both this problem and the reduction of data being successfully undertaken by Mrs. M. W. Jennings. Finally, I would like to thank Dr. T. P. Stecher for his interest in this work and especially for his helpful comments and criticisms.

TABLE 1

PHOTOMETER CHARACTERISTICS

	Photometer No. 1		Photometer No. 2	Background Detector
Detector	Bendix M310, Ser. No. 21		Bendix M310, Ser. No. 20	Bendix M310, Ser. No. 15
Filter	LiF		SrF_2	Aluminum
Telescope clear aperture	17.2 cm^2		17.3 cm^2	--
Telescope focal length	~ 6 inches		~ 6 inches	--
Field of view	1.92° circular		2.00° circular	--
Spectral band	1050Å < λ < 1650Å		1297Å < λ < 1650Å	--
Effective λ	1050 < λ < 1297 Lyman-α	1297 < λ < 1650A 1381Å	1376Å	--
System sensitivity	3.43×10^6 $ergs^{-1}$ cm^2 ster	2.66×10^{11} $ergs^{-1}$ cm^2 A	2.32×10^{11} $ergs^{-1}$ cm^2 A	Electrons of $E \gtrsim 2.2$ Mev Protons of $E \gtrsim 22$ Mev

TABLE 2

PHOTOMETRIC OBSERVATIONS

No.	HD	Name	Sp	V	B-V	Ref	v sin i km sec^{-1}	F(1376) x 10^{10} ergs cm^{-2} sec^{-1} A^{-1}	$(m_{1376} - V)_u$ MAG	$(m_{1376} - V)$ MAG	Notes
1	5394	γ Cas	B0 IV:e	2.41	-.11	1	--	105 ± 11	- 3.46 ± .10	- 4.91 ± .22	v,(a)
2	10144	α Eri	B5 IV	0.51	-.16	2	--	189 ± 19	- 2.19 ± .12	- 2.19 ± .12	
3	14228	φ Eri	B8 V	3.56	-.13	3	--	8.1 ± 2.0	- 1.83 ± .26	- 1.53 ± .28	
4	16582	δ Cet	B2 IV	4.06	-.21	1	20	18.5 ± 1.9	- 3.22 ± .12	- 3.45 ± .16	
5	18883	93 Cet	B7 III	5.63	--	4	--	2.02 ± .58	- 2.39 ± .28	--	
6	21364	ξ Tau	B8 V	3.74	-.08	1	--	4.48 ± .81	- 1.36 ± .20	- 1.44 ± .22	(b)
7	21790	v Eri	B8 V	4.73	-.09	1	72	2.09 ± .71	- 1.53 ± .33	- 1.53 ± .33	
8	22203	τ^5 Eri	B8 V	4.28	-.12	1	--	3.26 ± .63	- 1.56 ± .20	- 1.33 ± .22	
9	22470	20 Eri	A0p	5.22	-.14	3	--	1.15 ± .46	- 1.36 ± .40	- .30 ± .43	
10	22928	δ Per	B5 III	3.03	-.12	1	255	11.5 ± 2.8	- 1.68 ± .25	- 1.98 ± .27	
11	23363	24 Eri	B8	5.09	--	5	--	1.22 ± .51	- 1.30 ± .38	--	(c)
12	23300	--	B9	5.64	--	5	--	1.79 ± .51	- 2.27 ± .33	--	(c)
13	23466	u Tau	B3	5.36	--	5	145	3.05 ± .54	- 2.56 ± .17	--	2,(c)
14	24504	--	B6 V	5.34	--	6	300	1.95 ± .52	- 2.02 ± .26	--	(c)

TABLE 2 (continued)

No.	HD	Name	Sp	V	B-V	Ref	v sin i km sec^{-1}	F(1376) x 10^{10} ergs cm^{-2} sec^{-1} A-1	$(m_{1376} - V)_u$ MAG	$(m_{1376} - V)$ MAG	Notes
15	24760	ϵ Per	B0.5 V	2.89	-.18	1	--	66 ± 7	- 3.43 ± .12	- 4.20 ± .18	3
16	24912	ξ Per	O7	4.06	.01	1	210	11.3 ± 1.6	- 2.68 ± .18	- 5.20 ± .35	2
17	25204	λ Tau	B3 V	3.41	-.12	1	$\leq$ 110	15.5 ± 1.6	- 2.38 ± .14	- 2.99 ± .18	2, v
18	25340	35 Eri	B5 V	5.25	--	6	190	2.94 ± .56	- 2.41 ± .19	--	(c)
19	25940	υ Per	B3 Vp	4.04	-.06	1	250	5.5 ± 1.0	- 1.89 ± .24	- 2.96 ± .28	
20	26793	--	B8	5.15	--	5	--	1.40 ± .65	- 1.51 ± .38	--	(c)
21	26912	μ Tau	B3 V	4.30	-.05	1	80	4.05 ± 1.01	- 1.81 ± .27	- 2.96 ± .31	3
22	27192	b^2 Per	B2 IV	5.54	--	7	--	2.04 ± .50	- 2.31 ± .21	--	(c)
23	27563	d Eri	B5 III	5.72	--	4	--	2.06 ± .71	- 2.50 ± .31	--	(c)
24	29248	υ Eri	B2 III	3.92	-.21	1	40	22.9 ± 2.3	- 3.31 ± .11	- 3.54 ± .16	2, v
25	29335	49 Eri	B5	5.32	--	5	140	2.22 ± .63	- 2.18 ± .26	--	2 (c)
26	30211	μ Eri	B5 IV	4.02	-.16	1	190	8.2 ± .8	- 2.30 ± .12	- 2.30 ± .12	3
27	30836	π^4 Ori	B2 III	3.67	-.15	1	40	16.9 ± 2.1	- 2.74 ± .13	- 3.42 ± .18	2
28	30614	α Cam	O9.5 Ia	4.29	.03	1	0	4.82 ± .95	- 1.99 ± .20	- 4.28 ± .34	2

TABLE 2 (continued)

No.	HD	Name	Sp	V	B-V	Ref	v sin i km sec^{-1}	F(1376) x 10^{10} ergs cm^{-2} sec^{-1} A^{-1}	$(m_{1376} - V)_u$ MAG	$(m_{1376} - V)$ MAG	Notes
29	31237	π^5 Ori	B2 III	3.73	-.19	1	90	14.8 ± 1.5	- 2.65 ± .12	- 3.03 ± .17	v
30	32630	η Aur	B3 V	3.17	-.17	1	125	28.0 ± 2.8	- 2.78 ± .12	- 3.01 ± .16	3
31	34759	ρ Aur	B5 V	5.12	--	8	90	3.70 ± .86	- 2.53 ± .22	--	(c)
32	35165	--	B5p	6.12	--	5	--	1.60 ± .84	- 2.62 ± .48	--	(c)
33	35468	γ Ori	B2 III	1.64	-.23	1	60	165 ± 16	- 3.18 ± .14	- 3.26 ± .18	2
34	35497	β Tau	B7 III	1.66	-.13	1	82	62 ± 6	- 2.13 ± .12	- 2.06 ± .16	
35	35708	o Tau	B3 V	4.89	-.14	1	10	6.8 ± 1.0	- 2.96 ± .21	- 3.42 ± .24	3
36	36486	δ Ori	09.5 II	2.20	-.21	1	140	210 ± 21	- 4.00 ± .10	- 4.69 ± .16	
37	36653	35 Ori	B3	5.58	--	5	--	2.62 ± .77	- 2.62 ± .26	--	3(c)
38	37128	ε Ori	B0 Ia	1.70	-.19	1	85	170 ± 26	- 3.27 ± .18	- 3.65 ± .21	
39	37202	ζ Tau	B2 IVp	3.03	-.18	1	310	31.7 ± 3.2	- 2.78 ± .12	- 3.24 ± .17	4
40	37367	--	B2 V	6.00	--	7	--	1.61 ± .66	- 2.51 ± .42	--	(c)
41	37742	ζ Ori	09.5 Ia	1.74	-.21	1	120	130 ± 26	- 3.02 ± .13	- 3.48 ± .17	
42	37711	126 Tau	B3 IV	4.85	-.12	1	90	5.2 ± .7	- 2.63 ± .18	- 3.24 ± .22	2,D

TABLE 2 (continued)

No.	HD	Name	Sp	V	B-V	Ref	v sin i km sec^{-1}	F(1376) x 10^{10} ergs cm^{-2} sec^{-1} A^{-1}	$(m_{1376}$ - V$)_u$ MAG	$(m_{1376}$ - V) MAG	Notes
43	40183	β Aur	A2 V	1.90	.02	1	--	3.16 ± .85	.86 ± .29	1.16 ± .31	v,D,(d)
44	40312	θ Aur	B9.5p	2.63	-.08	1	48	3.49 ± .67	.02 ± .23	.40 ± .26	2v
45	45542	υ Gem	B7 IV	4.14	-.14	1	220	4.43 ± .72	- 1.75 ± .20	- 1.60 ± .22	2
46	46328	ξ CMa	B0.5 IV	4.35	-.25	1	--	22.7 ± 2.9	- 3.74 ± .15	- 3.96 ± .18	
47	47839	s Mon	O7	4.66	-.24	1	19	22.3 ± 4.4	- 4.03 ± .22	- 4.64 ± .25	
48	48879	42 Cam	B3 IV	5.04	--	6	140	4.05 ± .83	- 2.55 ± .20	--	(c)
49	49340	43 Cam	B7 IV	5.13	--	6	205	1.60 ± .52	- 1.64 ± .31	--	(c)
50	51309	ι CMa	B3 II	4.39	-.06	1	0	3.80 ± 1.12	- 1.83 ± .28	- 2.75 ± .32	
51	52918	19 Mon	B1 V	5.01	-.20	1	350	6.8 ± 1.2	- 3.09 ± .13	- 3.55 ± .17	
52	53244	γ CMa	B8 II	4.11	-.11	1	≤ 15	2.96 ± .82	- 1.28 ± .28	- .98 ± .30	
53	67880	--	B3	5.54	--	5	--	3.32 ± .74	- 2.84 ± .24	--	(c)
54	68520	ε Vol	B5 V	4.34	-.12	3	--	4.28 ± .67	- 1.91 ± .17	- 2.22 ± .20	
55	68273	γ^2 Vel	O7+WC7	1.82	-.27	1	--	248 ± 38	- 3.80 ± .26	- 4.18 ± .28	
56	71518	--	B5	6.55	--	5	--	1.58 ± .52	- 3.04 ± .30	--	(c)

TABLE 2 (continued)

No.	HD	Name	Sp	V	B-V	Ref	v sin i km sec^{-1}	F(1376) x 10^{10} ergs cm^{-2} sec^{-1} A^{-1}	$(m_{1376}$ - V$)_u$ MAG	$(m_{1376}$ - V) MAG	Notes
57	73390	e^1 Car	B3 V	5.25	-.15	3,7	--	3.02 ± .71	- 2.44 ± .25	- 2.83 ± .28	
58	74753	D Vel	B3n	5.15	-.22	3	--	9.1 ± 1.0	- 3.54 ± .14	- 3.39 ± .17	
59	74956	δ Vel	A0:V	1.94	-.04	1	--	2.86 ± .69	.93 ± .26	.62 ± .28	D
60	75311	f Car	B3 Vne	4.81	--	4,7	--	8.0 ± .8	- 3.06 ± .16	--	
61	76805	H Vel	B5 V	4.69	-.14	3	--	4.63 ± .79	- 2.35 ± .18	- 2.50 ± .21	
62	87901	α Leo	B7 V	1.35	-.12	1	352	44.1 ± 4.8	- 1.46 ± .13	- 1.46 ± .13	
63	81188	κ Vel	B2 IV	2.50	-.20	3	--	77 ± 8	- 3.22 ± .13	- 3.52 ± .17	
64	91465	p Car	B5 IV	3.30	-.11	2	--	16.2 ± 1.6	- 2.32 ± .16	- 2.70 ± .17	v
65	103287	γ UMa	A0 V	2.44	0	1	165	3.08 ± .59	.34 ± .26	.34 ± .26	2
66	105937	ρ Cen	B4 V	3.96	-.14	1	--	13.6 ± 1.4	- 2.79 ± .12	- 3.09 ± .16	
67	106911	β Cha	B5 IV	4.25	-.13	3	--	11.3 ± 1.4	- 2.87 ± .18	- 3.10 ± .21	v
68	108483	σ Cen	B2 V	3.91	-.20	1	--	20.8 ± 3.1	- 3.20 ± .16	- 3.50 ± .20	
69	109387	κ Dra	B7p	3.89	-.14	1	250	6.9 ± .7	- 1.98 ± .13	- 1.82 ± .17	2
70	109668	α Mus	B3 IV	2.70	-.20	2	--	75 ± 8	- 3.38 ± .12	- 3.38 ± .12	

TABLE 2 (continued)

No.	HD	Name	Sp	V	B-V	Ref	v sin i km sec^{-1}	F(1376) x 10^{10} ergs cm^{-2} sec^{-1} A^{-1}	$(m_{1376}$ - V$)_u$ MAG	$(m_{1376}$ - V) MAG	Notes
71	112185	ε UMa	A0p	1.78	-.03	1	30	5.33 ± .79	.41 ± .19	.64 ± .22	2,v
72	116658	α Vir	B1 V	.96	-.23	1	--	426 ± 43	- 3.53 ± .15	- 3.61 ± .18	
73	120315	η UMa	B3 V	1.86	-.19	1	210	99 ± 10	- 2.84 ± .12	- 2.92 ± .16	3
74	121263	ζ Cen	B2 IV	2.54	-.24	1	--	118 ± 12	- 3.72 ± .13	- 3.72 ± .13	
75	122451	β Cen	B1 II	.63	-.23	1	--	671 ± 82	- 3.69 ± .13	- 3.77 ± .16	D
76	125823	a Cen	B3 V	4.41	-.18	1	--	12.2 ± 1.6	- 3.12 ± .14	- 3.27 ± .18	
77	127972	η Cen	B1.5 Vne	2.30	-.21	1	--	92 ± 10	- 3.21 ± .13	- 3.51 ± .17	
78	129056	α Lup	B1 V	2.29	-.21	1	--	123 ± 12	- 3.51 ± .11	- 3.89 ± .16	
79	135742	β Lib	B8 V	2.61	-.11	1	230	8.5 ± 1.3	- .93 ± .18	- .78 ± .21	2
80	136298	δ Lup	B2 IV	3.21	-.22	1	--	57.5 ± 5.8	- 3.60 ± .12	- 3.76 ± .16	
81	138764	90 Lib	B6 IV	5.12	-.10	9	15	1.95 ± .60	- 1.84 ± .32	- 2.15 ± .34	
82	140436	γ CrB	A0 IV	3.85	-.01	1	100	1.35 ± .66	--	--	D
83	142669	ρ Sco	B2 V	3.85	-.20	1	180	23.2 ± 2.3	- 3.26 ± .12	- 3.56 ± .16	3
84	143018	π Sco	B1 V	2.92	-.19	1	--	57.3 ± 6.7	- 3.31 ± .12	- 3.84 ± .17	2

TABLE 2 (continued)

No.	HD	Name	Sp	V	B-V	Ref	v sin i km sec^{-1}	F(1376) x 10^{10} ergs cm^{-2} sec^{-1} A^{-1}	$(m_{1376} - V)_{MAG}$	$(m_{1376} - V)_{MAG}$	Notes
85	143275	δ Sco	B0 V	2.33	-.11	1	170	76 ± 8	- 3.03 ± .13	- 4.55 ± .24	2
86	145389	φ Her	B9p	4.27	-.07	1	0	2.33 ± .52	- 1.18 ± .22	- 1.11 ± .24	
87	147394	τ Her	B5 IV	3.89	-.15	1	20	8.4 ± .9	- 2.20 ± .13	- 2.28 ± .16	2
88	148703	N Sco	B2 IV	4.23	-.17	1	--	15.3 ± 1.7	- 3.19 ± .14	- 3.72 ± .18	
89	149630	σ Her	B9 V	4.20	-.02	1	285	1.06 ± .41	- .26 ± .36	- .57 ± .37	
90	149438	τ Sco	B0 V	2.82	-.25	1	< 20	118 ± 12	- 3.99 ± .13	- 4.38 ± .17	
91	149757	ζ Oph	09.5 V	2.56	.02	1	350	35.0 ± 3.5	- 2.41 ± .12	- 4.86 ± .17	3
92	156633	u Her	B3 + B3	4.83	-.15	1	--	6.8 ± .7	- 2.91 ± .10	- 3.29 ± .15	v,D
93	160762	ι Her	B3 V	3.80	-.18	1	0	16.4 ± 1.6	- 2.84 ± .09	- 2.99 ± .14	2
94	160578	κ Sco	B2 IV	2.41	-.18	1	--	109 ± 11	- 3.50 ± .12	- 3.96 ± .17	2
95	173948	λ Pav	B1 Ve	4.22	-.16	3	--	10.8 ± 1.1	- 2.80 ± .10	- 3.56 ± .17	
96	189103	θ^1 Sgr	B3 IV	4.35	-.15	3	--	10.4 ± 2.2	- 2.89 ± .23	- 3.27 ± .26	

Notes for TABLE 2

(a) A small letter v indicates a variable star. A capital D indicates a double star.

(b) According to Slettebak (1954) the Helium lines of this star are relatively broad and shallow indicating moderate axial rotation.

(c) The magnitude appearing in column 5 is the apparent visual magnitude of the Revised Harvard Photometry system.

(d) Slettebak (1954) reports little or no component of axial rotation in line of sight for this star.

References to TABLE 2

1. Iriarte, B., Johnson, H. L., Mitchell, R. I., and Wisniewski, W. K. 1965, Sky and Telescope, XXX, 21.

2. Northcott, R. J. 1962, Observers' Handbook, Royal Astronomical Society, Canada.

3. Royal Observatory Staff, Cape of Good Hope, 1961, Cape Mimeogram No. 12.

4. de Vaucouleurs, A. 1957, M. N., 117, 455.

5. Boss, B., and Collaborators 1937, General Catalogue, (Carnegie Institution of Washington).

6. Slettebak, A., and Howard, R. F. 1955, Ap. J., 121, 102.

7. Rubin, V. C. et al. 1962, Astron. J., 67, 491.

8. Stebbins, J. and Kron, G. E. 1956, Ap. J., 123, 440.

9. Bertiau, F. C. 1958, Ap. J., 128, 533.

TABLE 3

$E(m_{1376} - V)/E(B - V)$ For 8 Pairs of Stars

Star	Type	$X = \frac{E(m_{1376} - V)}{E(B - V)}$	Star	Type	$X = \frac{E(m_{1376} - V)}{E(B - V)}$
η UMa	B3 V	7.3 ± 2.2	ε Her	B3 V	7.8 ± 2.3
υ Per	B3 Vp		μ Tau	B3 V	
ε Her	B3 V	7.9 ± 2.3	η Aur	B3 V	8.1 ± 2.6
υ Per	B3 Vp		μ Tau	B3 V	
η Aur	B3V	8.1 ± 2.6	ζ Cen	B2 IV	7.6 ± 3.1
υ Per	B3 Vp		N Sco	B2 IV	
η UMa	B3 V	7.3 ± 2.2	τ Sco	BO V	6.9 ± 1.4
μ Tau	B3 V		δ Sco	BO V	

TABLE 4

The Mean Ultraviolet Color Index, $(\overline{m_{1376} - V})$, For 12 Spectral Types

No.	Star	Type	$(\overline{m_{1376} - V})$
17	ξ Per	O7	-4.83 ± 0.27
48	s Mon	O7	
37	δ Ori	O9.5 II	-4.69 ± 0.16
87	δ Sco	B0 V	-4.44 ± 0.08
94	τ Sco	B0 V	
16	ϵ Per	B0.5 V	-4.08 ± 0.12
47	ξ^1 CMa	B0.5 IV	
86	π Sco	B1 V	-3.87 ± 0.02
80	α Lup	B1 V	
66	κ Vel	B2 IV	-3.66 ± 0.05
77	ζ Cen	B2 IV	
85	ρ Sco	B2 V	
92	N Sco	B2 IV	
104	δ Lup	B2 IV	
36	o Tau	B3 V	-3.14 ± 0.07
101	θ^1 Sgr	B3 IV	
79	a Cen	B3 V	
73	α Mus	B3 IV	
31	η Aur	B3 V	
98	ι Her	B3 V	
76	η UMa	B3 V	
22	μ Tau	B3 V	
59	e^1 Car	B3 V	
55	ϵ Vol	B5 V	-2.28 ± 0.04
64	H Vel	B5 V	
91	τ Her	B5 IV	
2	α Eri	B5 IV	
27	μ Eri	B5 IV	
83	90 Lib	B6 IV	-2.14 ± 0.34
35	β Tau	B7 III	-1.95 ± 0.12
72	κ Dra	B7 V	

TABLE 4 (continued)

No.	Star	Type	$(\overline{m_{1376} - V})$
3	φ Eri	B8 V	
6	ξ Tau	B8 V	-1.43 ± 0.05
7	ν Eri	B8 V	
8	τ^5 Eri	B8 V	
89	φ Her	B9p	-1.11 ± 0.24

TABLE 5

Relationships Between Spectral Type and Temperature

Type MK	Effective Temperature (°K)		Type MK	Effective Temperature (°K)	
	Harris	Experimental		Harris	Experimental
O7	--	$34{,}000^{+13{,}000}_{-6{,}000}$	B5	16,400	13,300
O9.5	--	$29{,}500^{+7{,}000}_{-2{,}100}$	B6	15,400	12,800
B0	30,000	26,400 ± 900	B7	14,500	12,300
B0.5	--	23,200 ± 900	B8	13,400	11,000
B1	24,200	21,600	B9	12,400	10,200
B2	22,100	20,100	A0	10,800	8,800
B3	18,800	16,900			

FIGURE LEGENDS

Fig. 1 A simplified diagram of satellite 1964 83C. This satellite was magnetically stabilized with its magnetic axis parallel to the axis of symmetry. The optical axes of the ultraviolet radiation photometers are normal to the satellite magnetic axis. The dark areas in the Figure represent solar cell arrays.

Fig. 2 A simplified drawing of the ultraviolet photometer unit. Details may be found in the text.

Fig. 3 Graphs illustrating the absolute sensitivity as a function of wavelength for both photometers. Graph A shows this function for SrF_2 filtered photometer alone while graph B exhibits this function for both the LiF and SrF_2 filtered photometers together.

Fig. 4 Representative histograms of raw data which show the number of counts recorded in 1.23 seconds as a function of time. The abscissa is divided into units of twice the photometer accumulation period, 2.46 seconds.

Fig. 5 Average number of counts recorded by the stellar photometer per accumulation period when under calibration as a function of day number. The circles represent the experimental data, and the bars indicate the standard deviation. The solid line is based on the periodic calibration of a nearly identical photometer carried out in the laboratory.

Fig. 6 Flux values for 10 stars measured by the stellar photometer outside the earth's atmosphere plotted against the day on which the measurements were made. The bars indicate the standard deviation in the data.

Fig. 7 Extinction as a function of inverse wavelength. The open circles represent data from the paper of Boggess and Borgman (1964). The solid dot with error bars indicates the extinction and probable error at $\lambda 1376\text{Å}$ found in the present work. The solid curve is the theoretical curve No. 15 of van de Hulst (1949).

Fig. 8 Plot of the ultraviolet color index, $(m_{1376} - V)$, as a function of stellar spectral classification. Triangles represent stars with $v \sin i \geq 220$ km sec^{-1}. Circles represent stars of luminosity classes I and II. The numbers identify stars according to the running number of Table 2. The dashed lines indicate theoretical relationships based on the models of Mihalas (1964) for (a) log g = 4.5, (b) log g = 4.0, (c) log g = 3.5, (d) log g = 3.0, (e) log g = 2.0, and (f) log g = 1.0. The solid curve is based on the smoothed experimental temperature scale of Table 5.

Fig. 9 Plot of $10^4/T_e$ as a function of the intrinsic color index $(B - V)_o$. The effective temperature, T_e, is determined via the models of Mihalas (1964) from the mean color indices, $(\overline{m_{1376} - V})$, of Table 4.

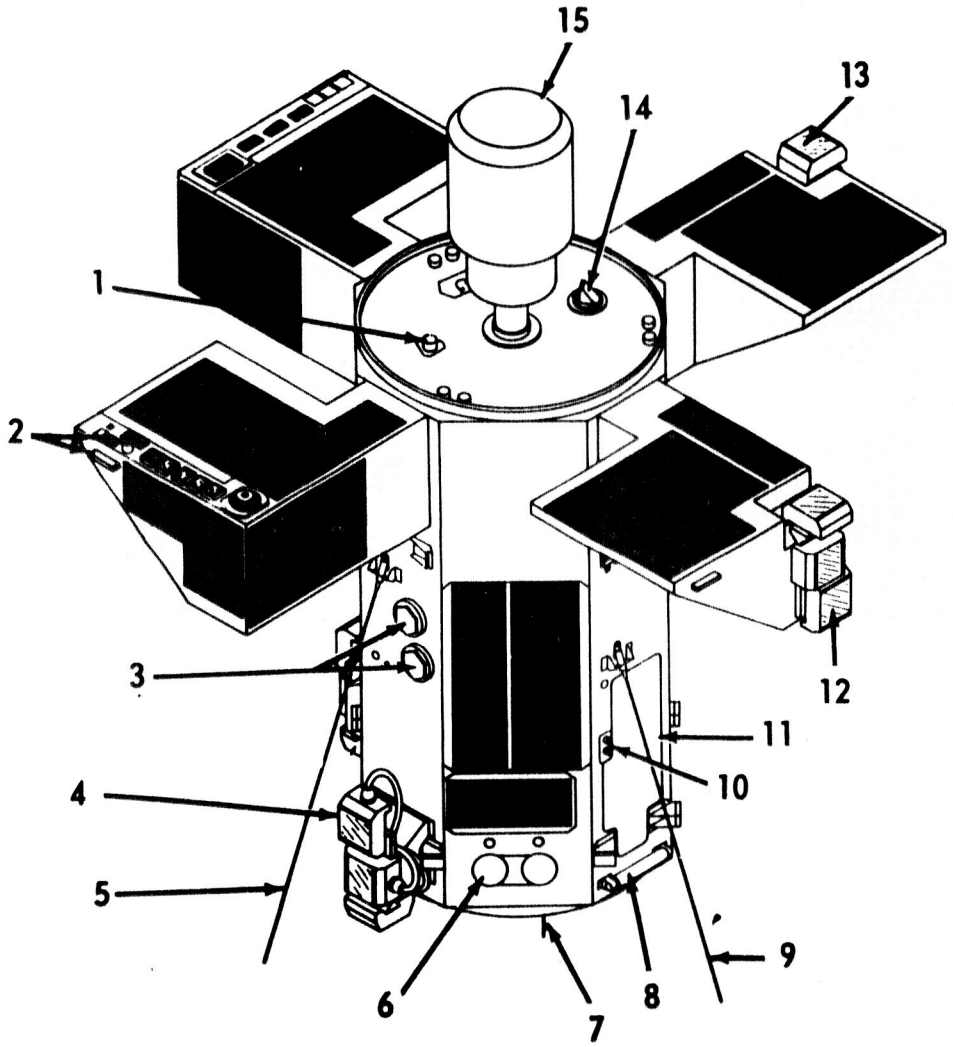

1. Z MAGNETOMETER SENSOR
2. SOLAR ATTITUDE DETECTORS
3. RELIABILITY EXPERIMENT
4. HELIOGONIOMETER
5. COMMAND RECEIVER ANTENNA
6. ULTRAVIOLET RADIATION PHOTOMETERS
7. 324 MC ANTENNA
8. Y MAGNETOMETER SENSOR
9. 162 MC ANTENNA
10. OMNI-DIRECTIONAL RADIATION DETECTORS
11. ACCESS PANEL
12. HELIOGONIOMETER
13. HELIOGONIOMETER
14. 4V BATTERY
15. RUBIDIUM VAPOR MAGNETOMETER BOOM ASSEMBLE

Fig. 1

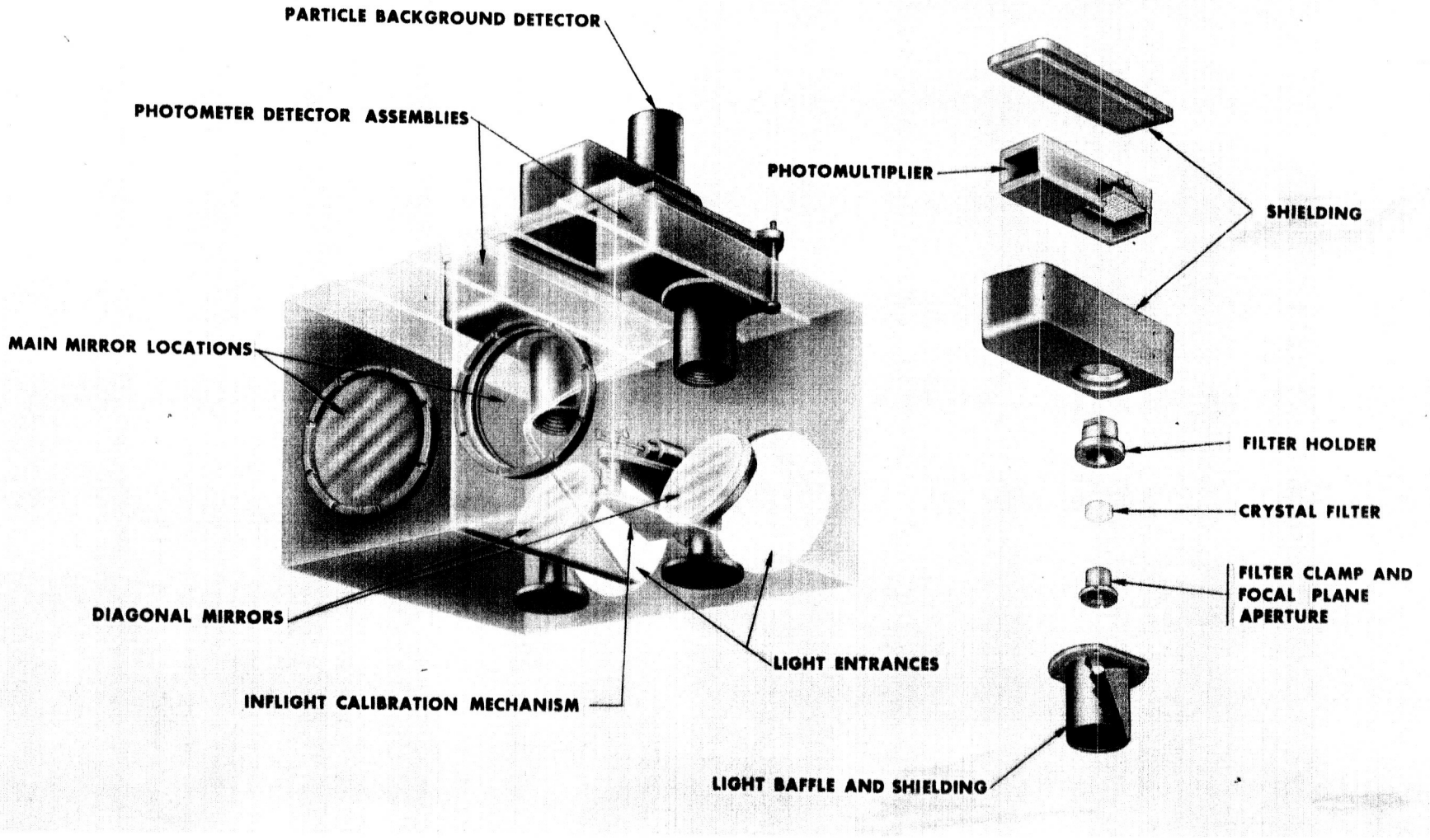

Fig. 2

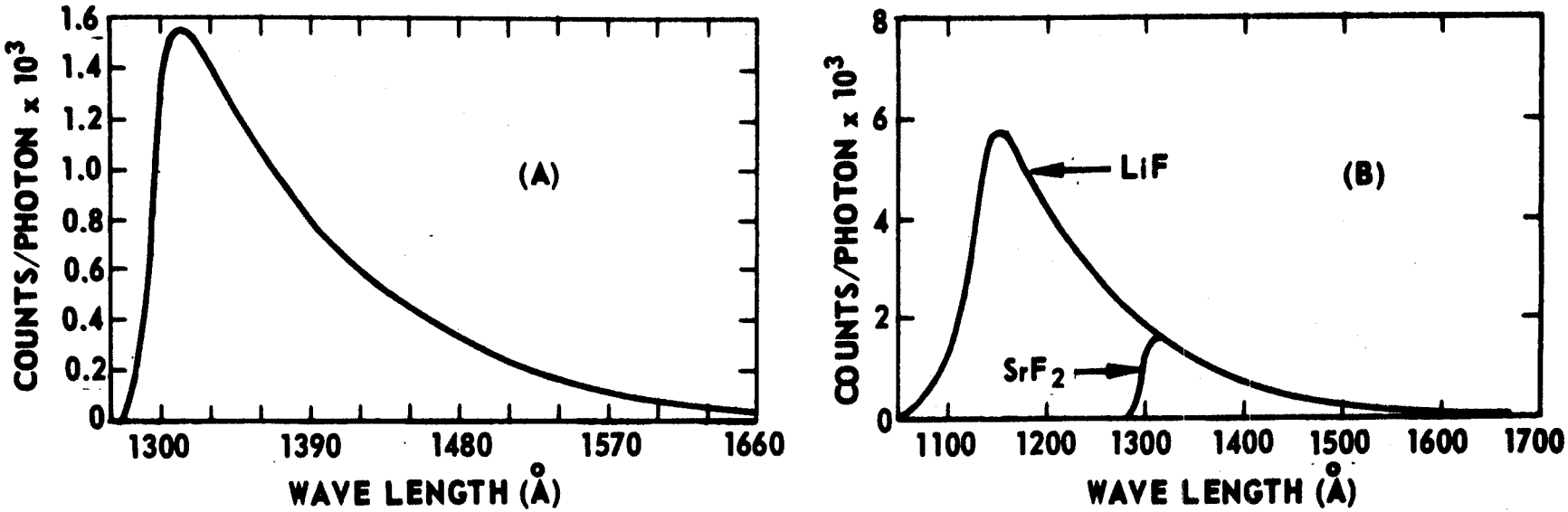
COUNTS/PHOTON x 10³
1.6
1.4
1.2
1.0
0.8
0.6
0.4
0.2
0
(A)
1300
1390
1480
1570
1660
WAVE LENGTH (Å)
COUNTS/PHOTON x 10³
8
6
4
2
0
LiF
(B)
SrF2
1100
1200
1300
1400
1500
1600
1700
WAVE LENGTH (Å)

Fig. 3

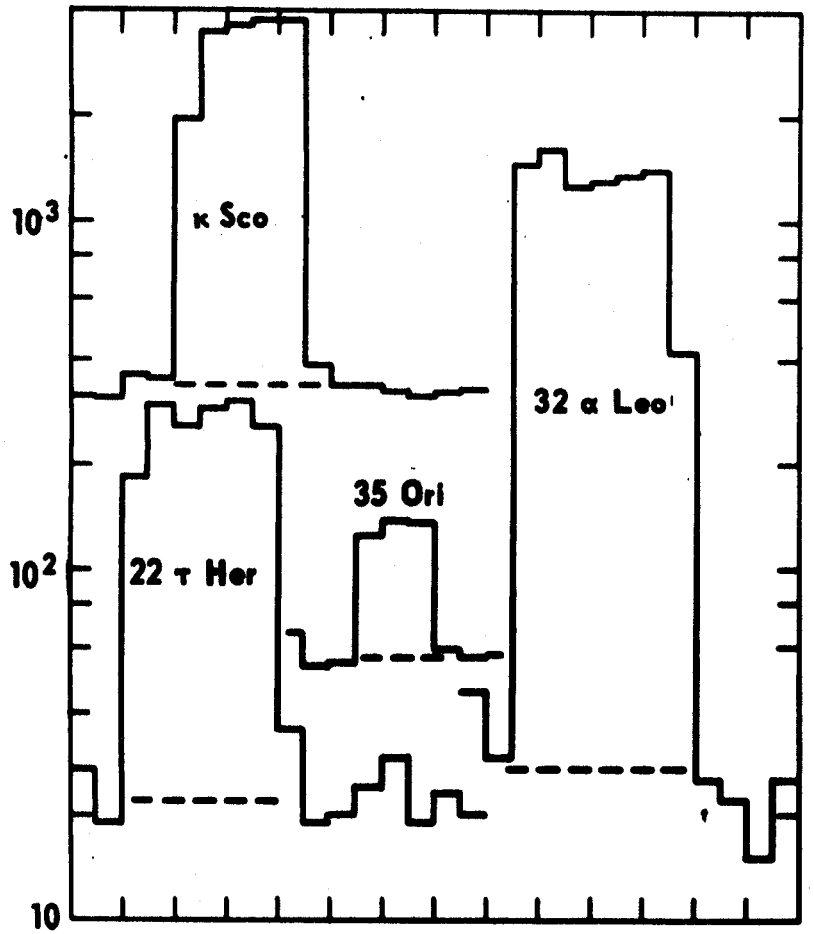
10^3
10^2
10
κ Sco
32 α Leo
35 Ori
22 τ Her

Fig. 4

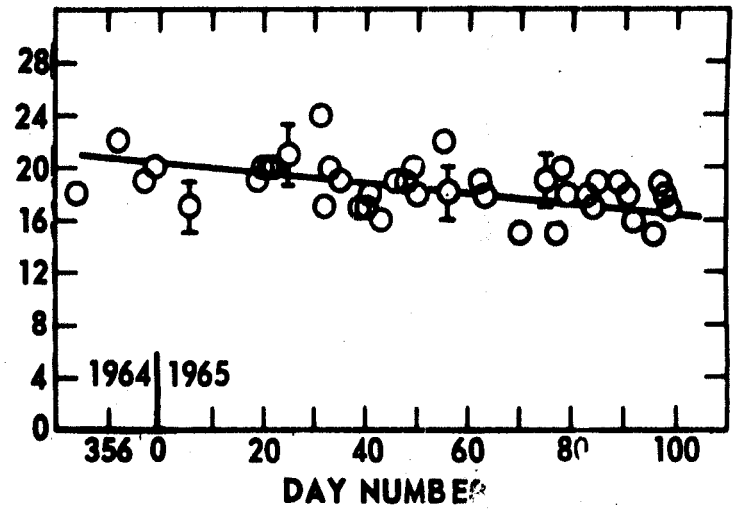
28
24
20
16
12
8
4
0
1964
1965
356
0
20
40
60
80
100
DAY NUMBER

Fig. 5

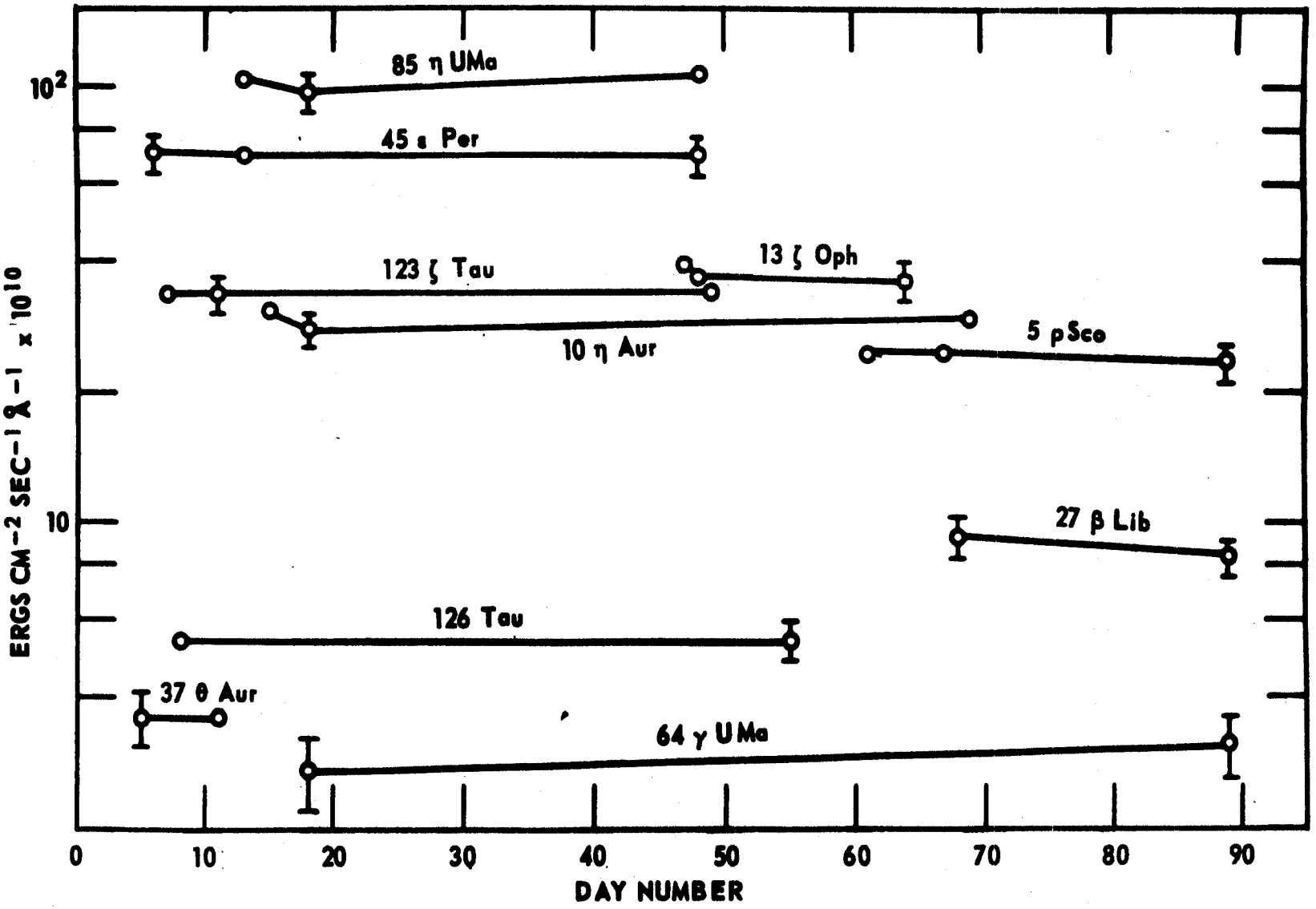
85 η UMa
45 ε Per
123 ζ Tau
13 ζ Oph
10 η Aur
5 ρ Sco
27 β Lib
126 Tau
37 θ Aur
64 γ UMa
10^2
10
ERGS CM^{-2} SEC^{-1} Å^{-1} x 10^{10}
0
10
20
30
40
50
60
70
80
90
DAY NUMBER

Fig. 6

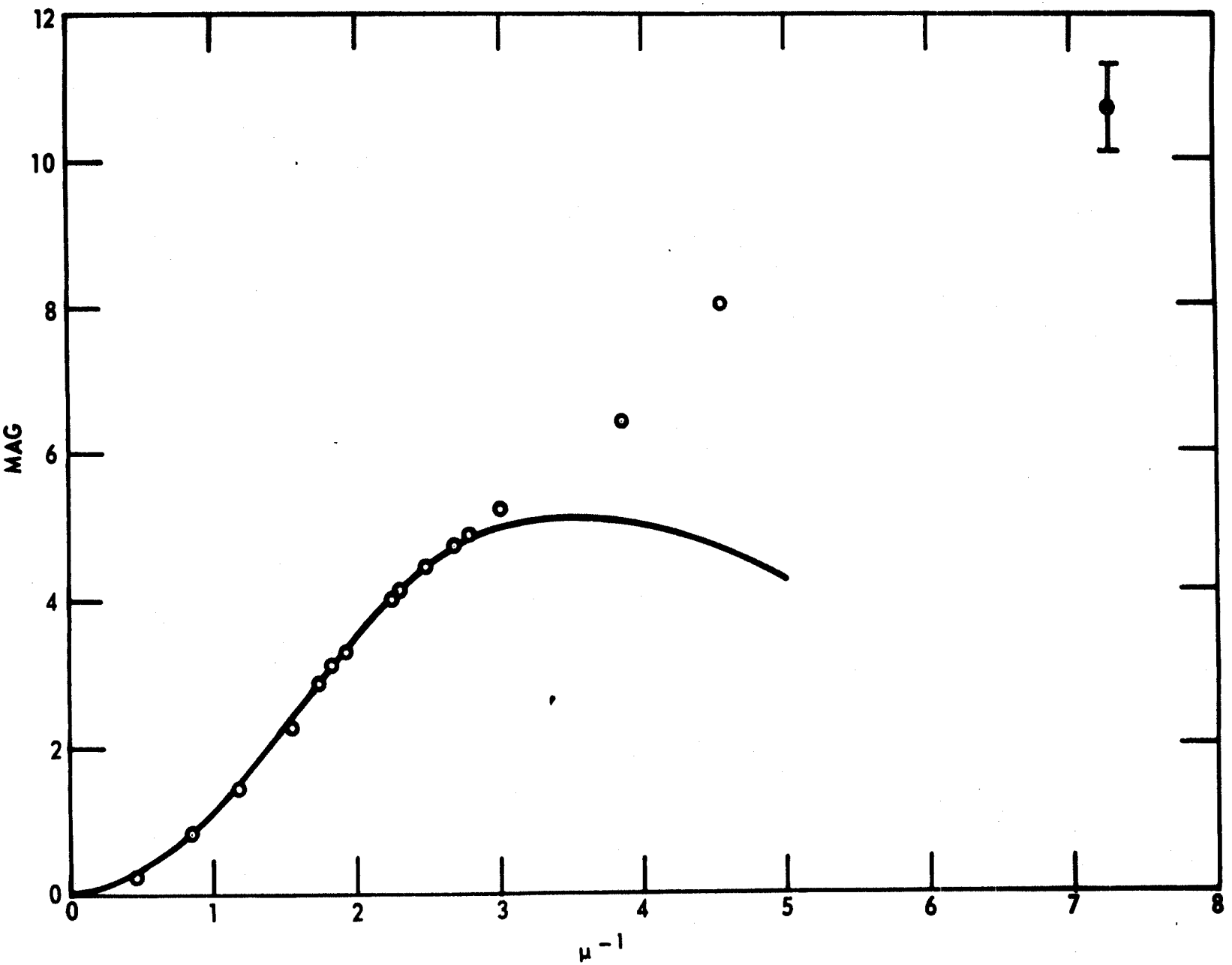

Fig. 7

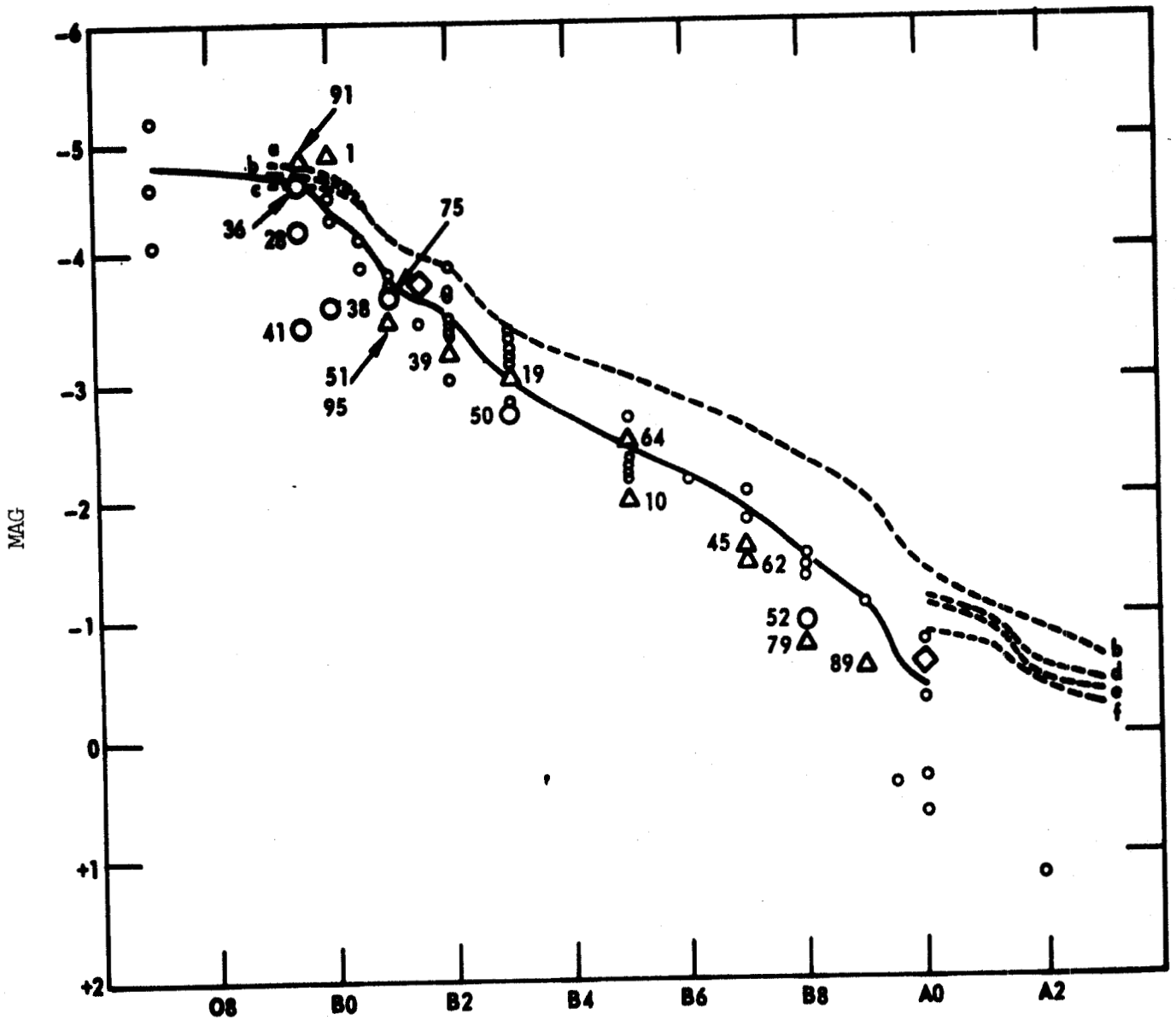
MAG
-6
-5
-4
-3
-2
-1
0
+1
+2
O8
B0
B2
B4
B6
B8
A0
A2
91
1
36
28
75
41
38
51
95
39
19
50
64
10
45
62
52
79
89
b
d
f

Fig. 8

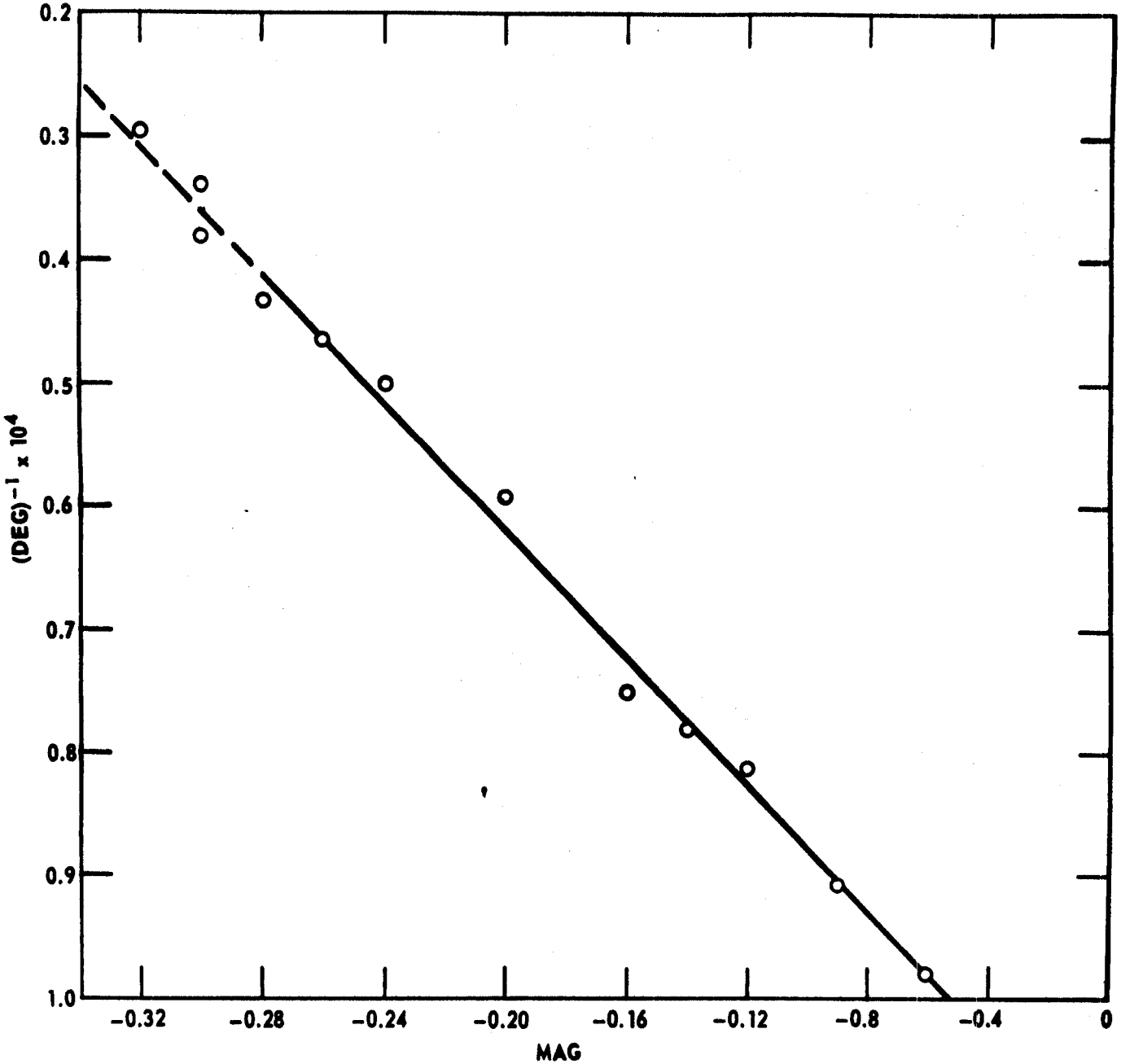
0.2
0.3
0.4
0.5
0.6
0.7
0.8
0.9
1.0
(DEG)$^{-1}$ x 10^4
-0.32
-0.28
-0.24
-0.20
-0.16
-0.12
-0.8
-0.4
0
MAG

Fig. 9

REFERENCES

Alexander, J. D. H., Bowen, P. J., and Heddle, D. W. O. 1963, Space Research III, ed. W. Priester (Amsterdam: North-Holland Publishing Co.), 1068.

Boggess III, A., and Borgman, J. 1964, Ap. J., 140, 1636.

Cain, J. C., Daniels, W. E., Hendricks, S. J., and Jensen, D. C. 1965, J. Geophys. Res., 70, 1940.

Chubb, T. A., and Byram, E. T. 1963, Ap. J., 138, 617.

Code, A. D. 1960, Stellar Atmospheres, ed. J. L. Greenstein (Chicago: University of Chicago Press), 50.

Collins II, G. W. 1965, Ap. J., 142, 265.

Goodrich, G. W., and Wiley, W. C. 1961, Rev. Sci. Instr., 32, 846.

Hanbury Brown, R., Hazard, C., Davis, J., Allen, L. R. 1964, Nature, 201, 1112.

Harris III, D. L. 1963, Basic Astronomical Data, ed. K. Aa. Strand (Chicago: University of Chicago Press), 263.

Hass, G., and Tousey, R. 1959, J. Opt. Soc. America, 41, 702.

Heroux, L., and Hinteregger, H. E. 1960, Rev. Sci. Instr., 31, 280.

Hulst, H. C. van de. 1949, Rech. Obs. Astr. Utrecht, II, Part 2.

Johnson, H. L. 1963, Basic Astronomical Data, ed. K. Aa. Strand (Chicago: University of Chicago Press), 204.

----------. 1965, Ap. J., 141, 923.

Mihalas, D. M. 1964, Ap. J. Suppl., 9, 321.

Mihalas, D. M., and Morton, D. C. 1965, Ap. J., 142, 253.

Samson, J. A. R. 1964, J. Opt. Soc. America, 54, 6.

Slettebak, A. 1949, Ap. J., 110, 498.

----------. 1954, Ap. J., 119, 146.

----------. 1955, Ap. J., 121, 102.

----------. 1956, Ap. J., 124, 173.

Stecher, T. P. 1964, A. J., 69, 558.

----------. 1965, Ap. J., 142, in press.

Stecher, T. P., and Donn, B. 1965, Ap. J., 142, in press.

Stecher, T. P., and Milligan, J. E. 1962, Ap. J., 136, 1.

Watanabe, K. 1954, J. Chem Phys., 22, 1564.

Wickramasinghe, N. C. 1963, M. N., 126, 99.